



Cite this: *CrystEngComm*, 2023, 25, 352

Received 10th November 2022,
 Accepted 23rd December 2022

DOI: 10.1039/d2ce01522f

rsc.li/crystengcomm

Microcrystal electron diffraction (MicroED) structure determination of a mechanochemically synthesized co-crystal not affordable from solution crystallization†

Toshiyuki Sasaki,^{‡*a} Takanori Nakane,^{‡b} Akihiro Kawamoto,^{‡b} Tomohiro Nishizawa,^{‡c} and Genji Kurisu^{‡*bde}

Solid-state grinding can provide “mechano-distinctive” co-crystals that are not accessible from solutions. Herein, we demonstrate the structure determination of a powdered mechano-distinctive co-crystal of 2-aminopyrimidine and succinic acid in a 2:1 molar ratio using microcrystal electron diffraction.

Solid-state grinding (SSG) or mechanochemical synthesis has become an increasingly common technique in the preparation of co-crystals.^{1–7} Co-crystallization by SSG has been applied to enhance dissolution, solubility, and bioavailability of many drugs in co-crystal engineering.^{8–10} In contrast to solution methods, SSG is ecofriendly and can be used for low-solubility compounds. Further, SSG can yield crystals with specific stoichiometries and crystal structures that are not attainable using solution methods.^{1,4,6} Consequently, SSG is an attractive and key technique in materials science.

The samples prepared by SSG are in a powder form comprising small crystals with sizes ranging from nano- to micrometers. These are too small for single-crystal X-ray diffraction (XRD), which is the most common technique used for crystal structure analyses. Powder XRD is an alternative technique for analyzing ground samples.¹¹ However, this

technique is susceptible to diffraction peak overlap due to coexistence of polymorphs and crystal-size-dependent peak broadening which hinders the analysis of the crystal structure.^{7,12}

Microcrystal electron diffraction (MicroED)^{13–18} is another technique for determining the structure of nano crystals based on electron microscopy. MicroED was initially developed for protein crystals^{19–21} but has been used for an increasing variety of small-molecule crystals in recent years.^{22–27} Very thin crystals show clear electron diffraction patterns owing to the strong interaction between electrons and matter, providing crystal structures directly from the powders.^{16,17,28} By exploiting this advantage, MicroED was applied to a ground co-crystal, whose structure was reported to be not accessible by the solution method in this study. Fig. 1 shows a representative example, focusing on a 2:1 co-crystal of 2-aminopyrimidine (2AP) and succinic acid (SA), which was first synthesized by Etter *et al.* in 1990.⁴

A 2:1 co-crystal in powder form was prepared for MicroED by grinding a 2:1 mixture of 2AP and SA using an agate mortar and pestle for 10 min. This sample was aged at 22–30 °C for nine days (ESI† Fig. S1†). Although the main component of the mixture was the 2:1 co-crystal after the aging, the diffraction peaks indicate existence of small amount of the 1:1 co-crystal ($2\theta = 11.8^\circ, 13.5^\circ$), 2AP ($2\theta = 18.5^\circ, 28.8^\circ, 29.6^\circ$) and SA ($2\theta = 26.2^\circ$). The powdered co-crystals were gently dusted on a copper EM grid (Quantifoil R1.2/1.3 Cu 200 mech) and loaded onto a Talos Arctica microscope (Thermo Fisher Scientific). Data collection was performed using SerialEM²⁹ with a strategy described in the

^a Department of Materials System Science, Yokohama City University, 22-2 Seto, Kanazawa-ku, Yokohama, Kanagawa 236-0027, Japan.

E-mail: tsasaki@yokohama-cu.ac.jp, t.devi.sasaki@gmail.com

^b Institute for Protein Research, Osaka University, 3-2 Yamadaoka, Suita, Osaka 565-0871, Japan. E-mail: gkurisu@protein.osaka-u.ac.jp

^c Department of Medical Life Science, Yokohama City University, 1-7-29 Suehiro-cho, Tsurumi-ku, Yokohama 230-0045, Japan

^d Department of Macromolecular Science, Graduate School of Science, Osaka University, Toyonaka 560-0043, Japan

^e Institute for Open and Transdisciplinary Research Initiatives, Osaka University, 2-1 Yamadaoka, Suita, Osaka 565-0871, Japan

† Electronic supplementary information (ESI) available: CCDC 2211429. For ESI and crystallographic data in CIF or other electronic format see DOI: <https://doi.org/10.1039/d2ce01522f>

‡ Contributed equally as co-first author.

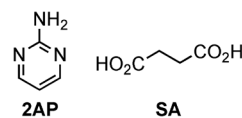


Fig. 1 Molecular structures of 2-aminopyrimidine (2AP) and succinic acid (SA).



literatures.^{23,24} Crystals were manually flagged on square atlases (Fig. 2) and diffraction patterns were automatically collected using Verlox controlled by SerialEM *via* AutoHotKeys. The dataset was collected under parallel illumination conditions at 200 kV, a gun lens 8, a spot size of 11 in the nanoprobe mode and with an electron dose rate of $0.05 \text{ e}^- \text{ \AA}^{-2} \text{ s}^{-1}$. With a $100 \text{ }\mu\text{m}$ condenser aperture and without a selected-area diffraction aperture, the beam diameter was approximately $1.35 \text{ }\mu\text{m}$. During data collection, the temperature of the specimen grid was maintained at 79 K . The diffraction patterns were recorded on a Ceta detector (CMOS $4\text{k} \times 4\text{k}$, Thermo Fisher Scientific) running at 1 frame per s, while the crystals were rotated by $60\text{--}70^\circ$ at 1° s^{-1} . Diffraction patterns were indexed, integrated, and scaled using DIALS.^{30–32} With a sample set in excess of 500 recorded crystals, diffraction patterns from 14 best crystals were merged to provide the final structure factors (ESI† Table S1). The crystal structure was solved using charge flipping and refined kinematically by SHELXL with Olex2 (ESI† Table S2).^{33–35} Owing to unmodeled dynamical scatterings and accuracy limitations of the virtual camera distance (618 mm), the standard deviations of the refined parameters are considered underestimated.

Both the 2:1 (this work) and 1:1 (refcode: SERMOR)⁴ co-crystal structures belong to the monoclinic space group $P2_1/c$ ($P2_1/n$), but they exhibit different molecular conformations and hydrogen-bonding networks, as seen in Fig. 3. In the 2:1 co-crystal, SA has a *trans* conformation and forms a ring-type hydrogen-bonding network with 2AP, which is denoted as $R_2^2(8)$ according to the graph-set analysis shown in Fig. 3a(i).^{36–39} Another ring-type hydrogen-bonding network of $R_2^2(8)$ is formed between neighboring 2AP. Consequently, the 2:1 co-crystal formed a zigzag ($\Psi = 57.1^\circ$) supramolecular tape with inversion centers at the centers of SA and a ring-type hydrogen-bonding network of 2AP. The tapes leaning against the *b*-axis stack along the *a*-axis to form a 2-dimensional (2D) supramolecular layer, as shown in Fig. 3b(i). The 3-dimensional (3D) crystal structure is an assembly of layers along the *c*-axis. Fig. 3a(ii) depicts the 1:1

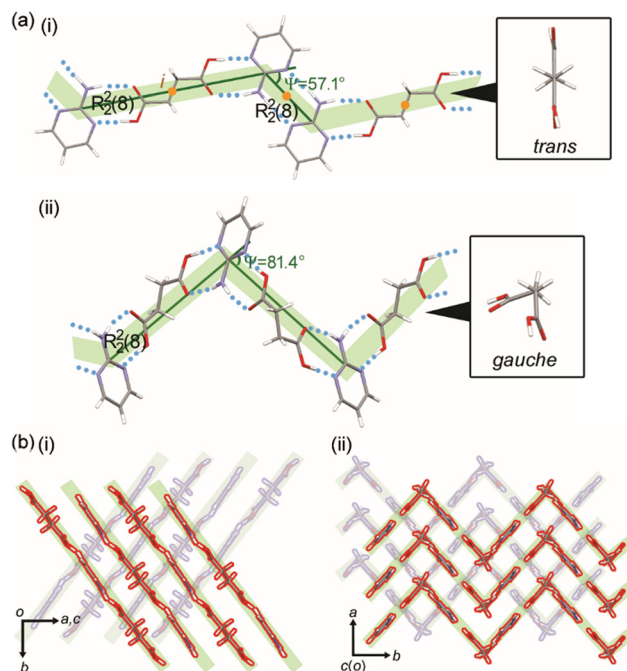


Fig. 3 (a) Hydrogen-bonding networks and (b) packing diagrams of the (i) 2:1 (this work) and (ii) 1:1 (refcode: SERMOR)⁴ co-crystals.

co-crystal forms, which form a zigzag ($\Psi = 81.4^\circ$) supramolecular tape with no inversion centers by ring-type hydrogen-bonding networks of $R_2^2(8)$ between SA with the *gauche* conformation and 2AP. 2D supramolecular layers constructed by stacking the tape along the *a*-axis yield a 3D crystal structure, as shown in Fig. 3b(ii).

The differences in the crystal structures and intermolecular interactions such as hydrogen-bonding networks can change the stability of the co-crystal as investigated by thermal analyses. The 2:1 co-crystal showed a 32% mass reduction starting at approximately 100°C owing to sublimation. It melted at 149°C in thermal measurements performed for thermogravimetric (TG) and differential thermal analysis (DTA), as seen in Fig. 4a and S2a.† $^1\text{H-NMR}$ spectroscopy showed that the sublimated solid was 2AP (Fig. S3†). However, the 1:1 co-crystal prepared by mixing 2AP and SA in a 1:1 molar ratio in ethanol had no peaks before the melting point of 149.5°C , similar to the peaks of the 2:1 co-crystal (Fig. S2b†). This indicates that the 2:1 co-crystal transforms into the 1:1 co-crystal by releasing 2AP. Fig. 4b shows that powder XRD confirmed the formation of 1:1 co-crystals (Fig. S1†). Diffraction peaks, *e.g.* at $2\theta = 17.7^\circ$, characteristic of the 1:1 co-crystal appeared when heating the 2:1 co-crystal at 120°C for 2 min. The co-crystals formed SA in addition to the remaining *ca.* 7 mol% of the 1:1 co-crystal, as determined by $^1\text{H-NMR}$ spectroscopy after heating for further 13 min (Fig. S4†). Moreover, the 2:1 co-crystals gradually transformed into 1:1 co-crystals when kept at room temperature. Fig. 4b and c show that approximately 80% of a batch of 2:1 co-crystals transformed into 1:1 co-crystals after 3 months (Fig. S5†). This shows that the 2:1 co-crystal has a

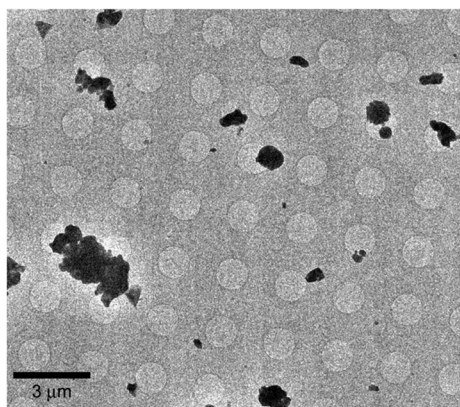


Fig. 2 Cryo-EM image of the 2:1 co-crystals.



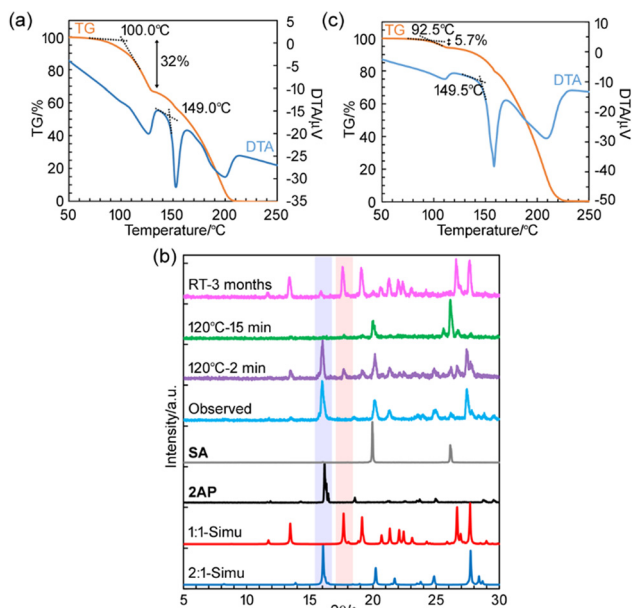


Fig. 4 (a) TG/DTA diagram of the 2:1 co-crystal. (b) Powder XRD patterns measured at 24 °C: simulated from the crystal structures of the 2:1 co-crystal (2:1-Simu, blue) and 1:1 co-crystal (1:1-Simu, red); experimental patterns of 2AP (2AP, black), SA (SA, gray), the 2:1 co-crystal before (Observed, light blue) and after heating for 2 (120 °C–2 min, purple) and 15 min (120 °C–15 min, green); and the 2:1 co-crystal after aging for 3 months under ambient conditions (RT–3 months, pink). Representative diffraction peaks of the 2:1 and 1:1 co-crystals are highlighted by blue and red, respectively. (c) TG/DTA diagram of the 2:1 co-crystal after aging for 3 months under ambient conditions.

lower stability than that of the 1:1 co-crystal under ambient conditions.

The stabilities of the co-crystals were further evaluated with regard to the theoretically calculated energies listed in Tables 1 and S3.† The crystal structures, which were solved based on different techniques, *i.e.* microcrystal electron and power X-ray diffraction,⁴ were optimized and their lattice energies (E_{lat}) were calculated using CONFLEX9 (MMFF94s).^{40,41} BSSE-corrected intermolecular interaction energies (E_{int}) between hydrogen-bonded molecules (2AP⋯2AP and 2AP⋯SA) were calculated at the B3LYP-D3/6-311G** level of theory^{42–44} using the counterpoise method⁴⁵ with Gaussian 16 (ref. 46) and Gauss view 6.0.16.⁴⁷ This was based on the dimers retrieved from the optimized crystal structures. The E_{lat} of the 2:1 co-crystal (-125.47 kcal mol⁻¹) indicates its lower stability than that of the 1:1 co-crystal (-182.97 kcal mol⁻¹). Further, while the supramolecular tape in the 1:1 co-crystal is constructed by a robust hydrogen-bonding network (E_{int} (2AP⋯SA) = -16.31 kcal mol⁻¹), both

Table 1 Lattice (E_{lat}) and intermolecular interaction (E_{int}) energies (kcal mol⁻¹)

Entry	E_{lat}	E_{int} (2AP⋯2AP)	E_{int} (2AP⋯SA)
2:1 co-crystal	-125.47	-12.36	-16.01
1:1 co-crystal	-182.97	—	-16.31

this network (E_{int} (2AP⋯SA) = -16.01 kcal mol⁻¹) and a relatively weak hydrogen-bonding network (E_{int} (2AP⋯2AP) = -12.36 kcal mol⁻¹) are formed in the 2:1 co-crystal.

In conclusion, the co-crystal structure of 2AP and SA in a 2:1 molar ratio synthesized by SSG are not accessible by solution methods. This precludes the preparation of large single crystals suitable for structure determination by single-crystal XRD. However, the crystal structure of the 2:1 co-crystal was determined using MicroED. Although more accurate atomic positions of the 2:1 co-crystal might have been obtained by dynamical refinement, we limited our analysis to kinematical treatment due to technical difficulties. Kinematical refinement affords atomic positions accurate enough to discuss crystal packings. The 2:1 and 1:1 co-crystals of 2AP and SA have different stabilities owing to their different hydrogen-bonding networks and crystal structures, as determined by the thermal analyses and theoretical calculations. This demonstrates that MicroED is suitable to determine the crystal structure of powdered samples including those produced exclusively by SSG, or which are “mechano-distinctive”, and is useful in co-crystal engineering where SSG is a prevalent preparation method.

The refined structure of the 2:1 co-crystal was deposited to CCDC (accession code: 2211429) and COD (accession code: 3000424). The raw MicroED diffraction images were deposited to XRDa (accession code: XRD-109, <https://doi.org/10.51093/xrd-00109>). Input and output files for computational chemistry calculations and powder X-ray diffraction data were deposited to Zenodo (<https://doi.org/10.5281/zenodo.7435859>).

Author contributions

G. K. supervised this study. T. S. designed the project, prepared the samples, carried out theoretical calculations, and wrote the manuscript. T. N., A. K., T. N., and G. K. conducted MicroED experiments. All authors contributed to the discussion and manuscript review.

Conflicts of interest

There are no conflicts to declare.

Acknowledgements

This work was supported by JSPS KAKENHI Grant Number 22K05054 and Hitachi Metals–Materials Science Foundation for T. S. and Research Support Project for Life Science and Drug Discovery (BINDS) from AMED under Grant Number JP22ama121001. We thank Dr. Yanagisawa and Dr. Yamashita for their advice on semi-automatic MicroED data collection with SerialEM macros. We are also grateful to Dr. Suzuki for pre-evaluation of nanocrystals for MicroED by a fluorescence microscope and to Dr. Irie for measurements and analyses of ¹H-NMR spectra.



Notes and references

- 1 A. O. Patil, D. Y. Curtin and I. C. Paul, *J. Am. Chem. Soc.*, 1984, **106**, 348–353.
- 2 A. O. Patil, D. Y. Curtin and I. C. Paul, *J. Am. Chem. Soc.*, 1984, **106**, 4010–4015.
- 3 F. Toda, K. Tanaka and A. Sekikawa, *J. Chem. Soc., Chem. Commun.*, 1987, 279–280.
- 4 M. C. Etter and D. A. Adsmond, *J. Chem. Soc., Chem. Commun.*, 1990, 589–591.
- 5 A. V. Trask, D. A. Haynes, W. D. S. Motherwell and W. Jones, *Chem. Commun.*, 2006, 51–53.
- 6 A. V. Trask and W. Jones, *Top. Curr. Chem.*, 2005, **254**, 41–70.
- 7 T. Frišćić and W. Jones, *Cryst. Growth Des.*, 2009, **9**, 1621–1637.
- 8 M. R. Cairra, L. R. Nassimbeni and A. F. Wildervanck, *J. Chem. Soc., Perkin Trans. 2*, 1995, 2213–2216.
- 9 J. F. Remenar, S. L. Morissette, M. L. Peterson, B. Moulton, J. M. MacPhee, H. R. Guzmán and Ö. Almarsson, *J. Am. Chem. Soc.*, 2003, **125**, 8456–8457.
- 10 R. Thakuria, A. Delori, W. Jones, M. P. Lipert, L. Roy and N. Rodríguez-Hornedo, *Int. J. Pharm.*, 2013, **453**, 101–125.
- 11 E. Y. Cheung, S. J. Kitchin, K. D. M. Harris, Y. Imai, N. Tajima and R. Kuroda, *J. Am. Chem. Soc.*, 2003, **125**, 14658–14659.
- 12 J. A. Kaduk, S. J. L. Billinge, R. E. Dinnebier, N. Henderson, I. Madsen, R. Černý, M. Leoni, L. Lutterotti, S. Thakral and D. Chateigner, *Nat. Rev. Methods Primers*, 2021, **1**, 77.
- 13 B. L. Nannenga and T. Gonen, *Nat. Methods*, 2019, **16**, 369–379.
- 14 M. J. de la Cruz, J. Hattne, D. Shi, P. Seidler, J. Rodriguez, F. E. Reyes, M. R. Sawaya, D. Cascio, S. C. Weiss, S. K. Kim, C. S. Hinck, A. P. Hinck, G. Calero, D. Eisenberg and T. Gonen, *Nat. Methods*, 2017, **14**, 399–402.
- 15 C. G. Jones, M. W. Martynowycz, J. Hattne, T. J. Fulton, B. M. Stoltz, J. A. Rodriguez, H. M. Nelson and T. Gonen, *ACS Cent. Sci.*, 2018, **4**, 1587–1592.
- 16 M. Gemmi, E. Mugnaioli, T. E. Gorelik, U. Kolb, L. Palatinus, P. Boullay, S. Hovmöller and J. P. Abrahams, *ACS Cent. Sci.*, 2019, **5**, 1315–1329.
- 17 X. Mu, C. Gillman, C. Nguyen and T. Gonen, *Annu. Rev. Biochem.*, 2021, **90**, 431–450.
- 18 Z. Huang, E. S. Grape, J. Li, A. K. Inge and X. Zou, *Coord. Chem. Rev.*, 2021, **427**, 213583.
- 19 B. L. Nannenga, D. Shi, A. G. W. Leslie and T. Gonen, *Nat. Methods*, 2014, **11**, 927–930.
- 20 K. Yonekura, K. Kato, M. Ogasawara, M. Tomita and C. Toyoshima, *Proc. Natl. Acad. Sci. U. S. A.*, 2015, **112**, 3368–3373.
- 21 D. Shi, B. L. Nannenga, M. G. Iadanza and T. Gonen, *eLife*, 2013, **2**, e01345.
- 22 T. Gruene, J. T. C. Wennmacher, C. Zaubitzer, J. J. Holstein, J. Heidler, A. Fecteau-Lefebvre, S. De Carlo, E. Müller, K. N. Goldie, I. Regeni, T. Li, G. Santiso-Quinones, G. Steinfeld, S. Handschin, E. van Genderen, J. A. van Bokhoven, G. H. Clever and R. Pantelic, *Angew. Chem., Int. Ed.*, 2018, **57**, 16313–16317.
- 23 H. Hamada, T. Nakamuro, K. Yamashita, H. Yanagisawa, O. Nureki, M. Kikkawa, K. Harano, R. Shang and E. Nakamura, *Bull. Chem. Soc. Jpn.*, 2020, **93**, 776–782.
- 24 H. Lu, T. Nakamuro, K. Yamashita, H. Yanagisawa, O. Nureki, M. Kikkawa, H. Gao, J. Tian, R. Shang and E. Nakamura, *J. Am. Chem. Soc.*, 2020, **142**, 18990–18996.
- 25 M. Ueda, T. Aoki, T. Akiyama, T. Nakamuro, K. Yamashita, H. Yanagisawa, O. Nureki, M. Kikkawa, E. Nakamura, T. Aida and Y. Itoh, *J. Am. Chem. Soc.*, 2021, **143**, 5121–5126.
- 26 C. Guzmán-Afonso, Y.-L. Hong, H. Colaux, H. Iijima, A. Saitow, T. Fukumura, Y. Aoyama, S. Motoki, T. Oikawa, T. Yamazaki, K. Yonekura and Y. Nishiyama, *Nat. Commun.*, 2019, **10**, 3537–3546.
- 27 E. T. Broadhurst, H. Xu, S. Parsons and F. Nudelman, *IUCrJ*, 2021, **8**, 860–866.
- 28 D. Marchetti, F. Guagnini, A. E. Lanza, A. Pedrini, L. Righi, E. Dalcanale, M. Gemmi and C. Massera, *Cryst. Growth Des.*, 2021, **21**, 6660–6664.
- 29 D. N. Mastronarde, *J. Struct. Biol.*, 2005, **152**, 36–51.
- 30 G. Winter, D. G. Waterman, J. M. Parkhurst, A. S. Brewster, R. J. Gildea, M. Gerstel, L. Fuentes-Montero, M. Vollmar, T. Michels-Clark, I. D. Young, N. K. Sauter and G. Evans, *Acta Crystallogr., Sect. D: Struct. Biol.*, 2018, **74**, 85–97.
- 31 M. T. B. Clabbers, T. Gruene, J. M. Parkhurst, J. P. Abrahams and D. G. Waterman, *Acta Crystallogr., Sect. D: Struct. Biol.*, 2018, **74**, 506–518.
- 32 J. Beilsten-Edmands, G. Winter, R. Gildea, J. Parkhurst, D. Waterman and G. Evans, *Acta Crystallogr., Sect. D: Struct. Biol.*, 2020, **76**, 385–399.
- 33 O. V. Dolomanov, L. J. Bourhis, R. J. Gildea, J. A. K. Howard and H. Puschmann, *J. Appl. Crystallogr.*, 2009, **42**, 339–341.
- 34 L. J. Bourhis, O. V. Dolomanov, R. J. Gildea, J. A. K. Howard and H. Puschmann, *Acta Crystallogr., Sect. A: Found. Adv.*, 2015, **71**, 59–75.
- 35 G. M. Sheldrick, *Acta Crystallogr., Sect. C: Struct. Chem.*, 2015, **71**, 3–8.
- 36 M. C. Etter, J. C. MacDonald and J. Bernstein, *Acta Crystallogr., Sect. B: Struct. Sci., Cryst. Eng. Mater.*, 1990, **46**, 256–262.
- 37 M. C. Etter, *Acc. Chem. Res.*, 1990, **23**, 120–126.
- 38 J. Bernstein, R. E. Davis, L. Shimoni and N.-L. Chang, *Angew. Chem., Int. Ed. Engl.*, 1995, **34**, 1555–1573.
- 39 T. Sasaki, Y. Ida, I. Hisaki, T. Yuge, Y. Uchida, N. Tohna and M. Miyata, *Chem. – Eur. J.*, 2014, **20**, 2478–2487.
- 40 H. Goto, S. Obata, N. Nakayama and K. Ohta, *CONFLEX 8*, CONFLEX Corporation, Tokyo, Japan, 2017.
- 41 T. A. Halgren, *J. Comput. Chem.*, 1996, **17**, 490–519.
- 42 A. D. Becke, *J. Chem. Phys.*, 1993, **98**, 5648–5652.
- 43 C. Lee, W. Yang and R. G. Parr, *Phys. Rev. B*, 1988, **37**, 785–789.
- 44 S. Grimme, J. Antony, S. Ehrlich and H. Krieg, *J. Chem. Phys.*, 2010, **132**, 154104.
- 45 S. F. Boys and F. Bernardi, *Mol. Phys.*, 1970, **19**, 553–566.



- 46 M. J. Frisch, G. W. Trucks, H. B. Schlegel, G. E. Scuseria, M. A. Robb, J. R. Cheeseman, G. Scalmani, V. Barone, G. A. Petersson, H. Nakatsuji, X. Li, M. Caricato, A. V. Marenich, J. Bloino, B. G. Janesko, R. Gomperts, B. Mennucci, H. P. Hratchian, J. V. Ortiz, A. F. Izmaylov, J. L. Sonnenberg, D. Williams-Young, F. Ding, F. Lipparini, F. Egidi, J. Goings, B. Peng, A. Petrone, T. Henderson, D. Ranasinghe, V. G. Zakrzewski, J. Gao, N. Rega, G. Zheng, W. Liang, M. Hada, M. Ehara, K. Toyota, R. Fukuda, J. Hasegawa, M. Ishida, T. Nakajima, Y. Honda, O. Kitao, H. Nakai, T. Vreven, K. Throssell, J. A. Montgomery, Jr., J. E. Peralta, F. Ogliaro, M. J. Bearpark, J. J. Heyd, E. N. Brothers, K. N. Kudin, V. N. Staroverov, T. A. Keith, R. Kobayashi, J. Normand, K. Raghavachari, A. P. Rendell, J. C. Burant, S. S. Iyengar, J. Tomasi, M. Cossi, J. M. Millam, M. Klene, C. Adamo, R. Cammi, J. W. Ochterski, R. L. Martin, K. Morokuma, O. Farkas, J. B. Foresman and D. J. Fox, *Gaussian 16, Revision C.01*, Gaussian, Inc., Wallingford, CT, 2019.
- 47 R. D. Dennington II, T. A. Keith and J. M. Millam, *GaussView 6.0.16*, SemicheM, Inc., 2000–2016.

